

Supplementary Information

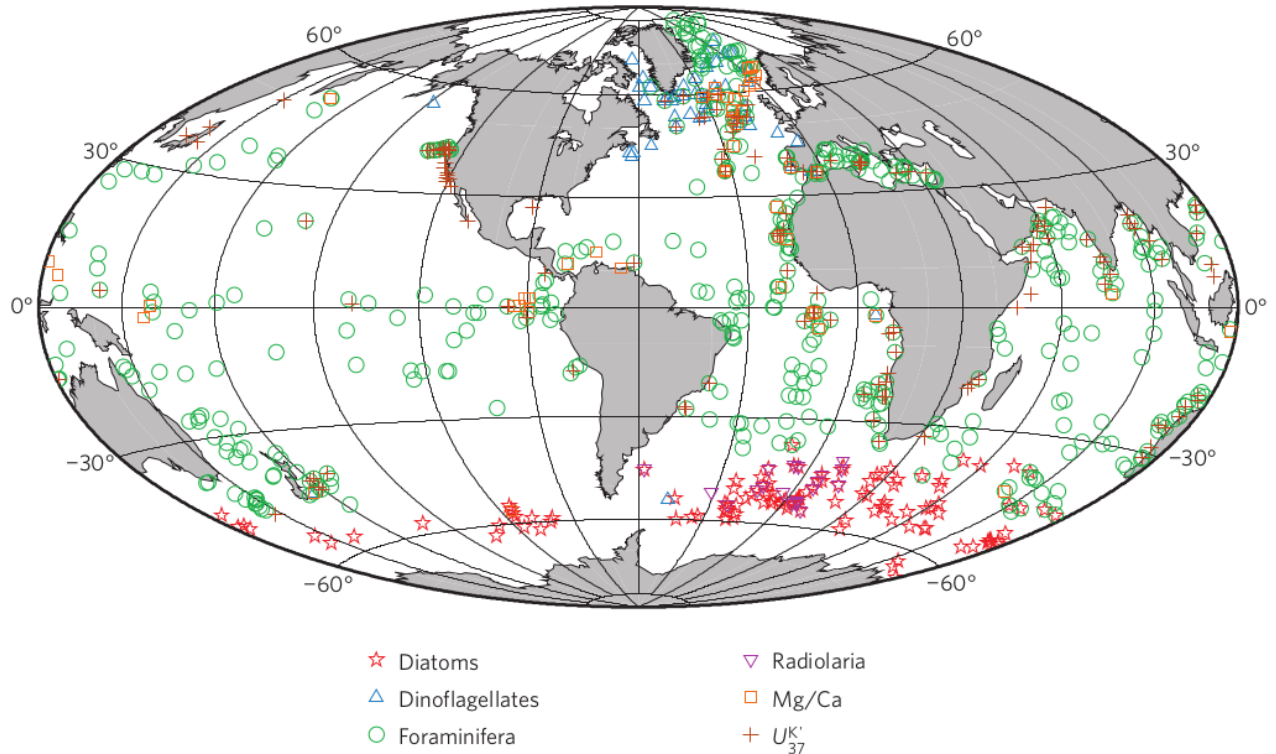


Fig. S1: Distribution of MARGO data points, indicating also which proxy was measured at each location (Waelbroeck et al., 2009).

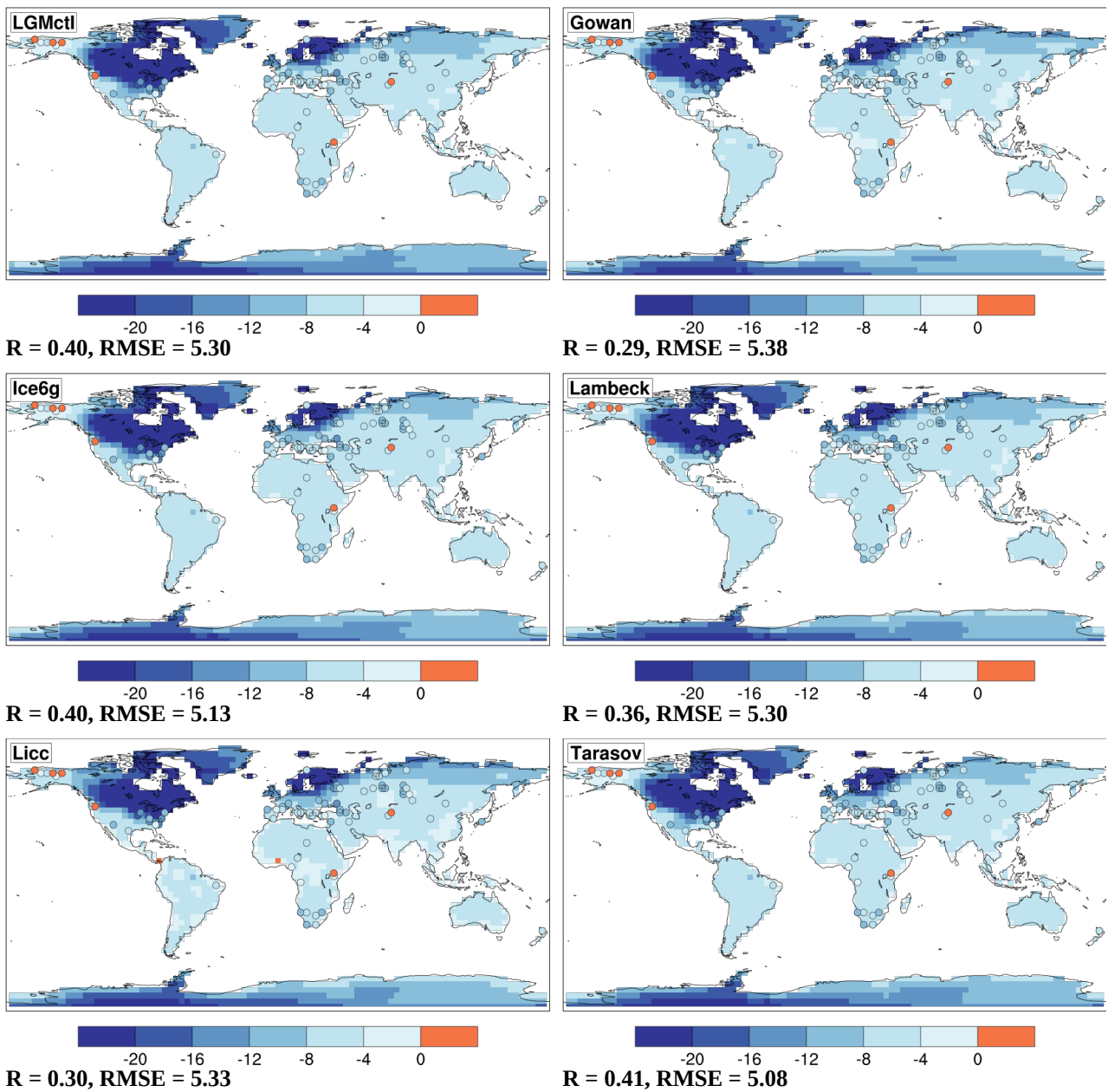


Fig. S2: Background color fill: simulated global pattern of annual mean surface temperature over land (T_{2m}) changes between the LGMctl and five ice sheet reconstructions and PI climate. The circles localize the pollen-based reconstructed temperature changes by Bartlein et al. (2011).

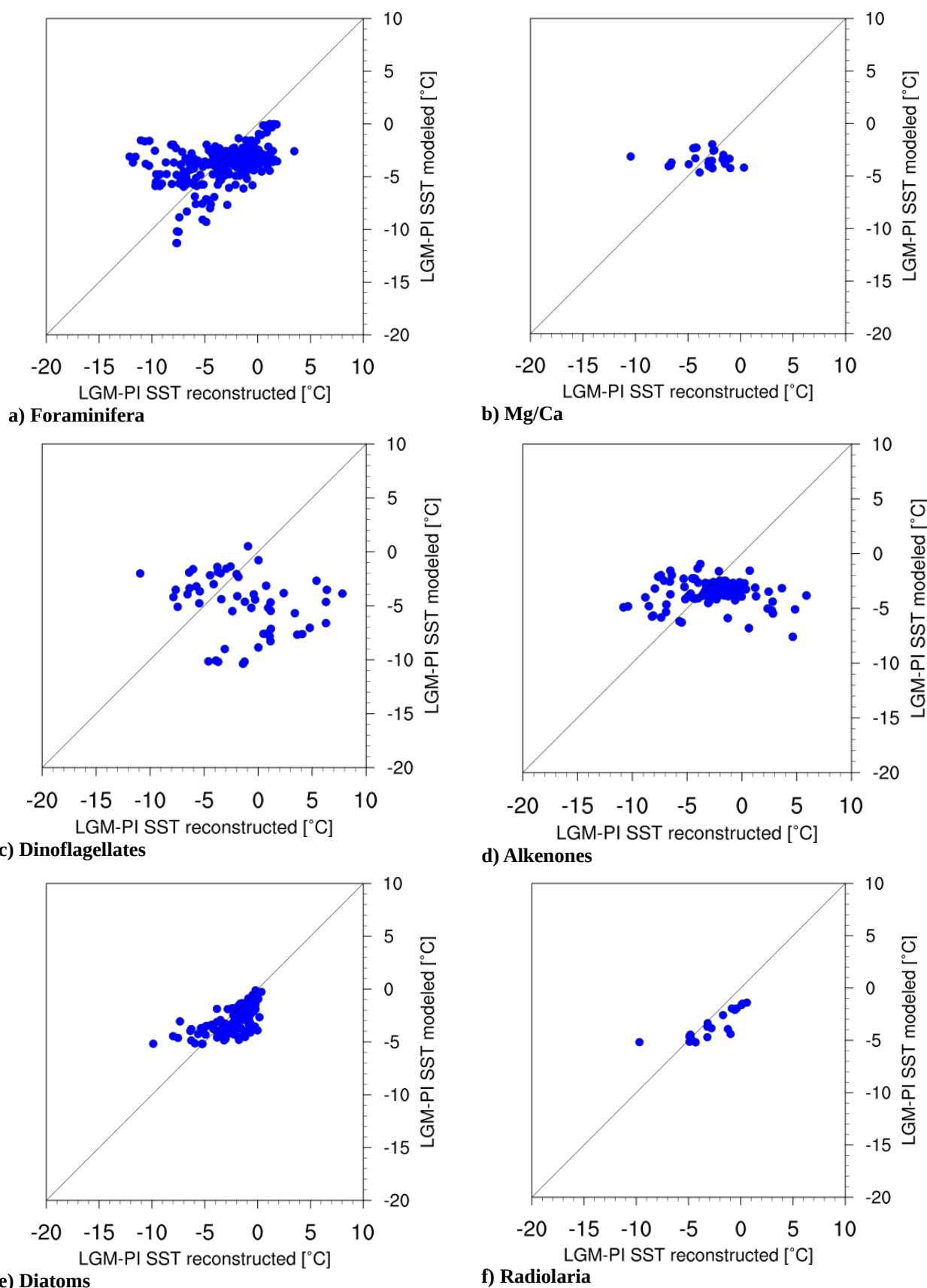
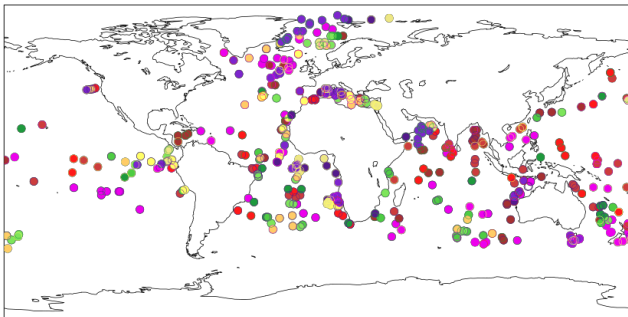
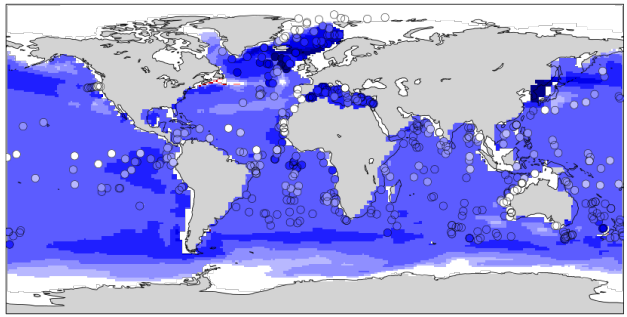


Fig. S3: Model fit: Comparison of reconstructed temperature changes of the annual mean LGM LIS experiment output vs. the simulated LGM-PI temperature at the sample locations based on planktonic foraminifera (a), Mg/Ca (b), dinoflagellates (c), alkenones (U^{37}) (d), diatoms (e) and radiolaria (f) reconstructions of MARGO project. The black line represents the 1:1 line indicating a perfect model fit.

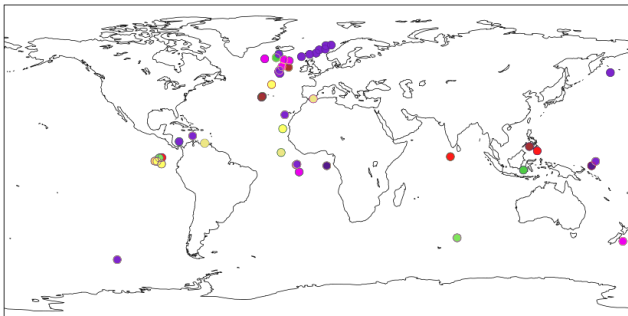
LGMctl vs Foraminifera Depth-Season Best Fit Data



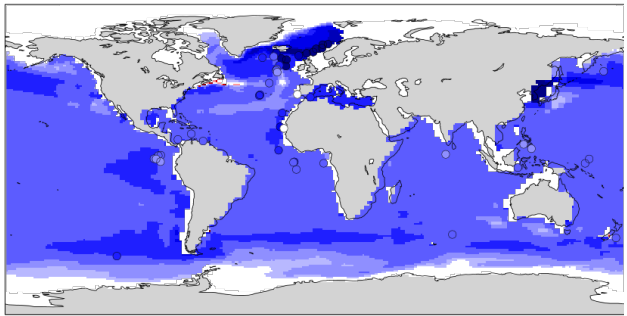
LGMctl vs Fora Seasonal-Depth Best Fit SST



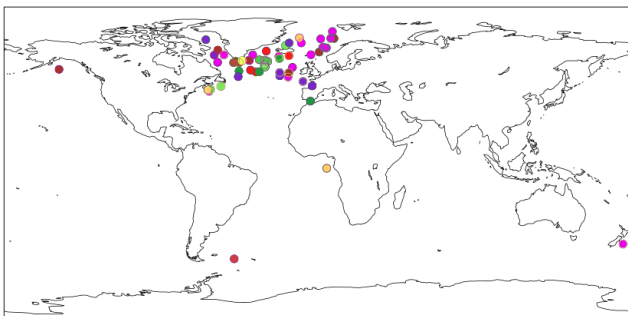
LGMctl vs MgCa Depth-Season Best Fit Data



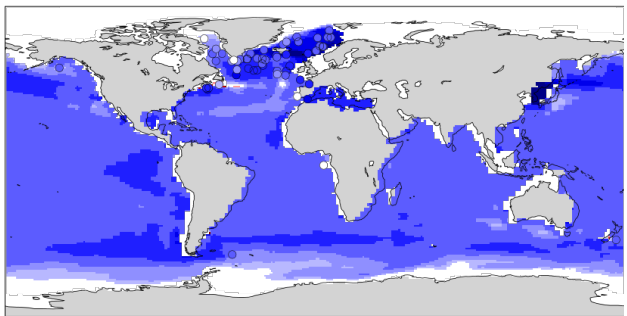
LGMctl vs Mgca Seasonal-Depth Best Fit SST



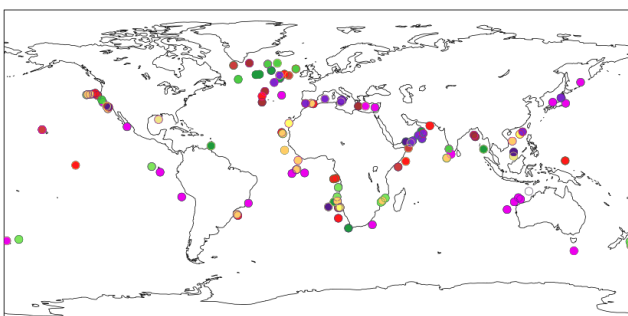
LGMctl vs Dinoflagellates Depth-Season Best Fit Data



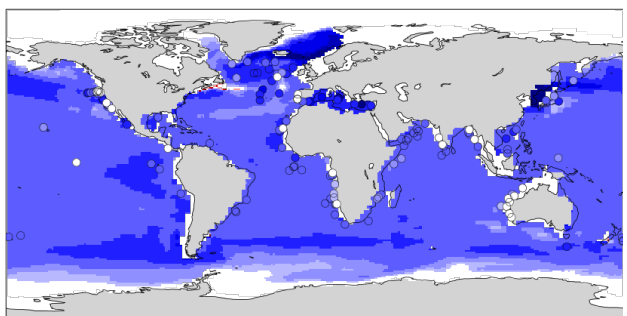
LGMctl vs Dino Seasonal-Depth Best Fit SST



LGMctl vs UK37 Depth-Season Best Fit Data



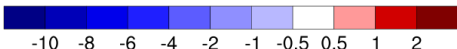
LGMctl vs UK37 Seasonal-Depth Best Fit SST



a)

Fig. S4: (a) The circles localize the foraminifera, Mg/Ca, dinoflagellates and $U^{k_{37}}$ records and the colors fill of the circles represent the different depth (m) mean in which the reconstruction agrees best with model. Border of the circles represent the different seasonal/annual mean in which the reconstruction agrees best with model (b) Background color fill: simulated global pattern of annual mean sea surface temperature changes between the LGM and PI climate. Color fill of the circles show the temperature change recorded by corresponding depth mean shown in (a) at the sample locations.

b)



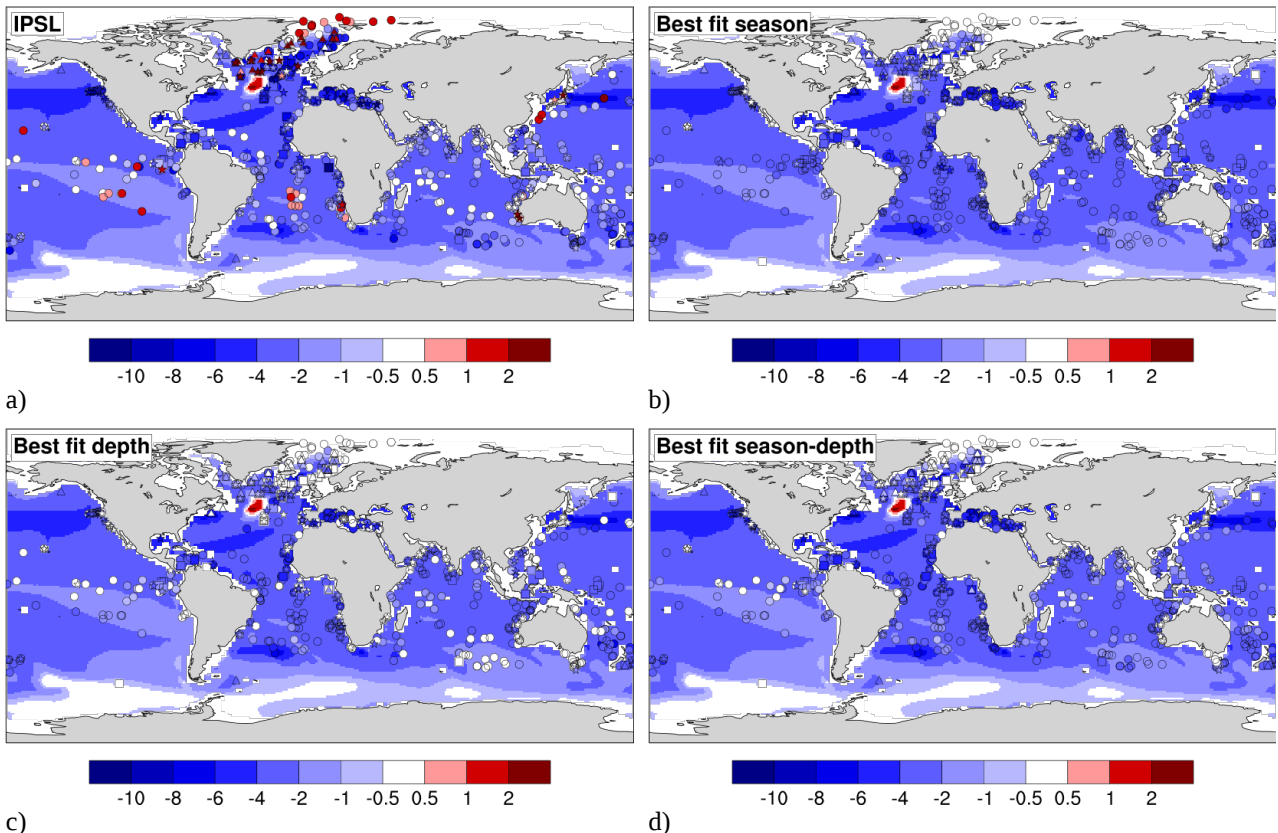


Fig. S5: (a) Global reconstructed SST trends of four proxies compared to simulated annual mean SST anomalies of IPSL-CM5A-LR. The colors fill of the circles represent the temperature anomalies as recorded by MARGO proxies records. (b) Best fit season of the model with proxies (c) Best fit depth (d) Best fit season and depth. Background color fill: simulated global pattern of annual mean sea surface temperature changes between the LGM and PI climate.

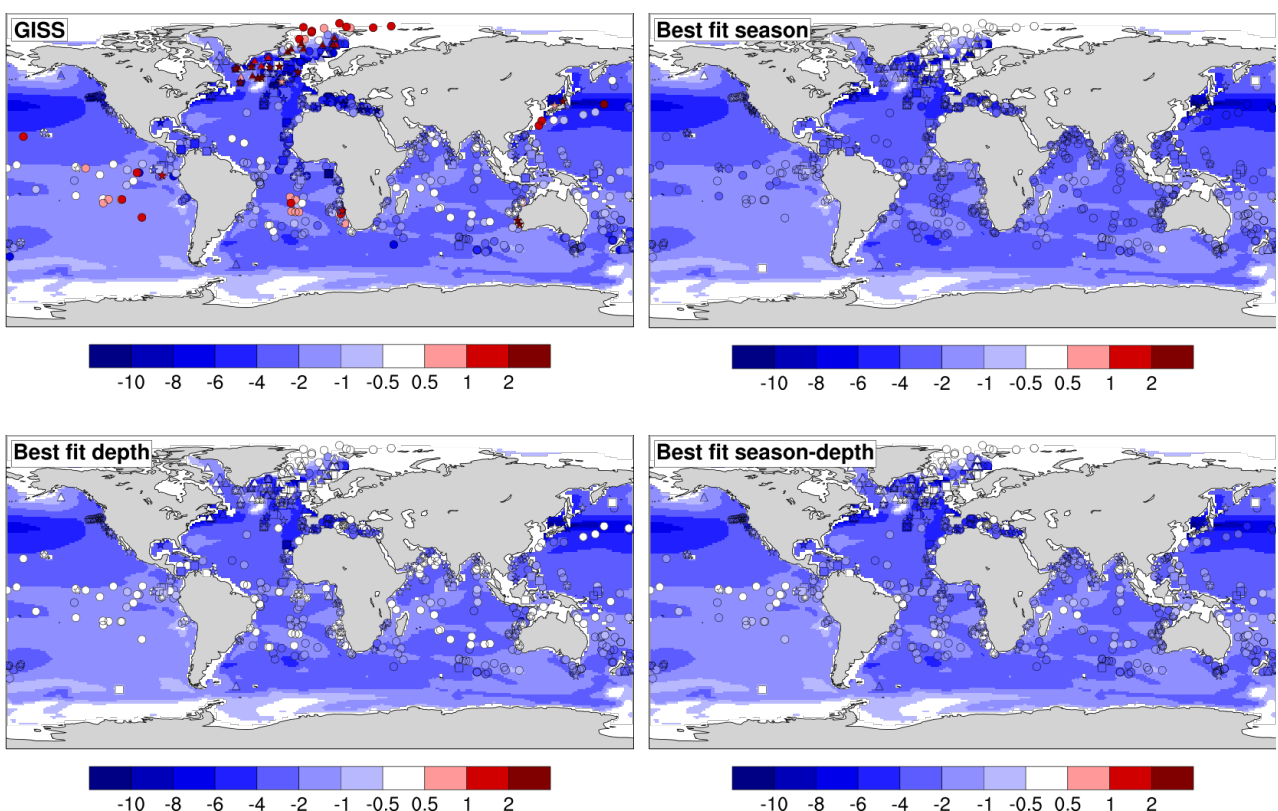


Fig. S6: As Fig. S5, but for GISS-E2.

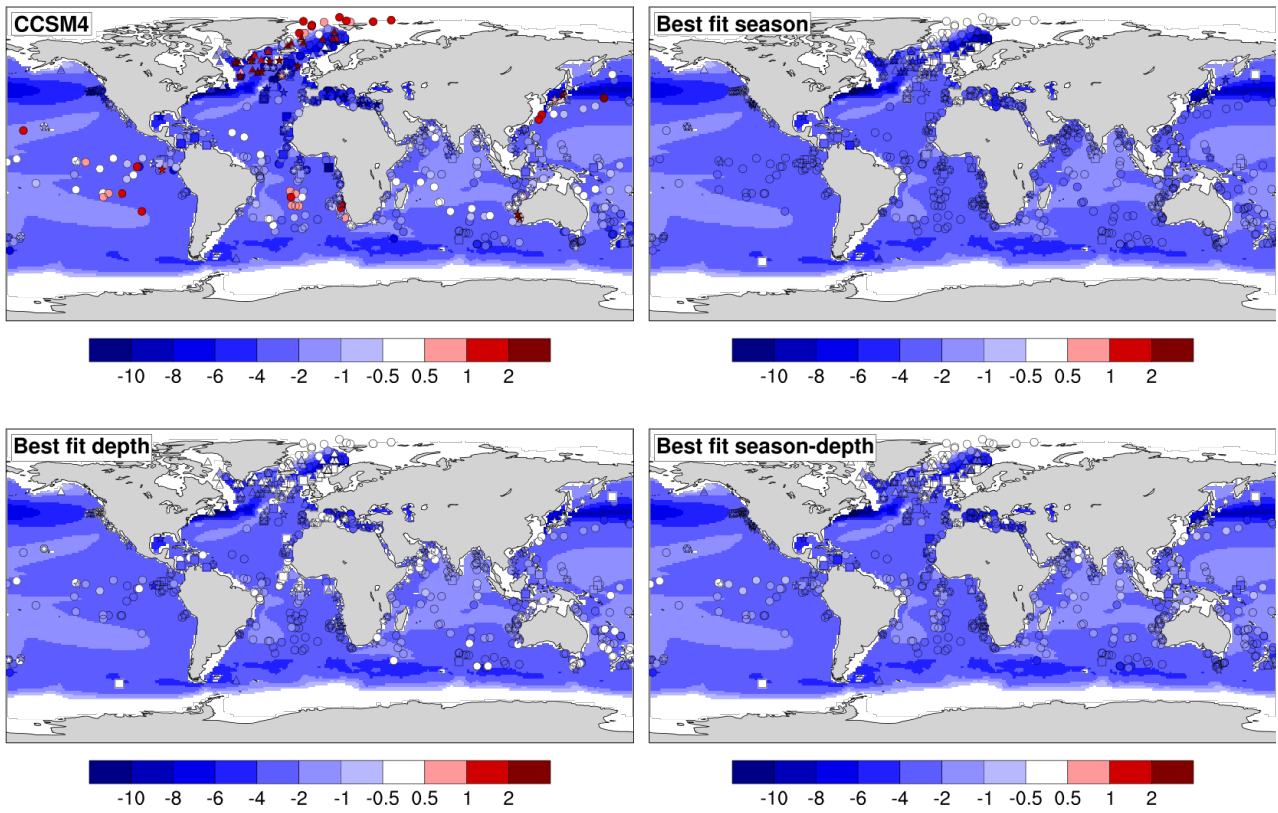


Fig. S7: As Fig. S5, but for CCSM4.

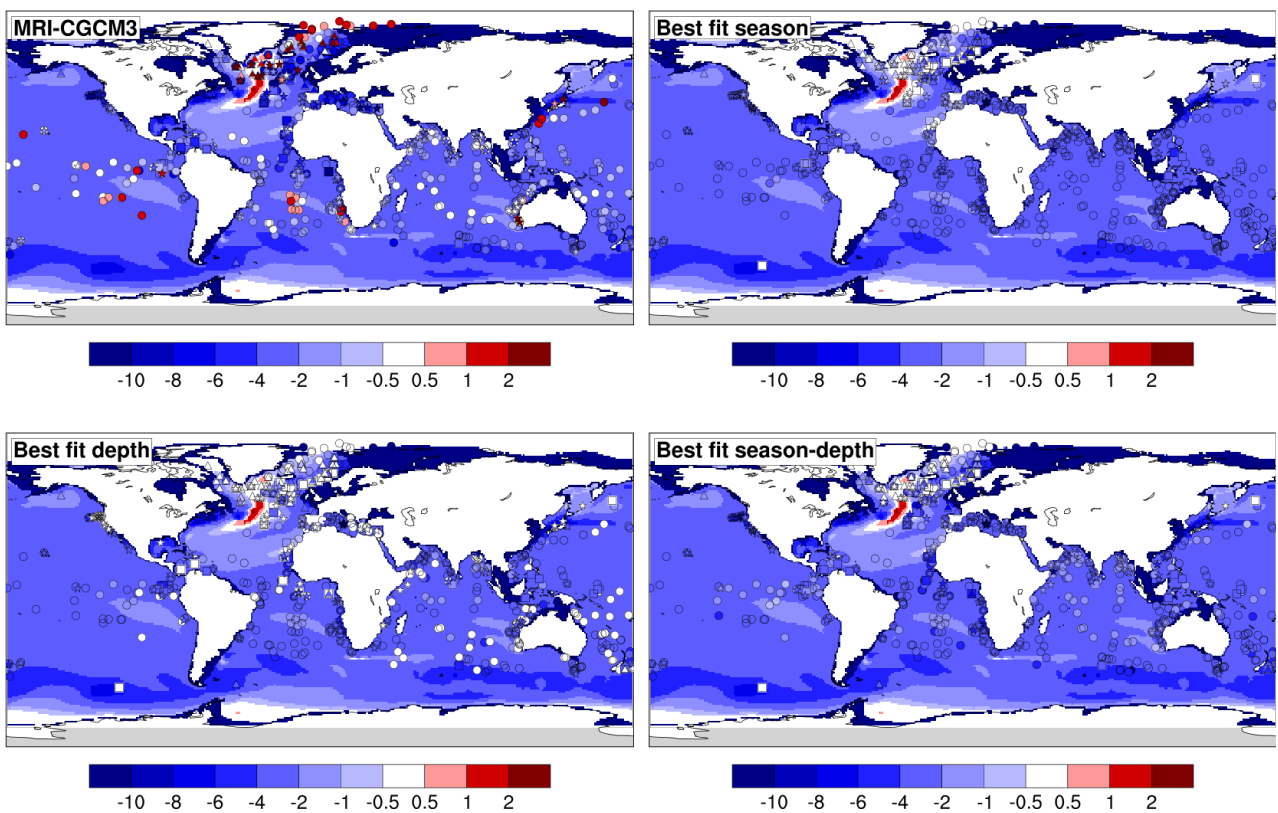


Fig. S8: As Fig. S5, but for MRI-CGCM3.

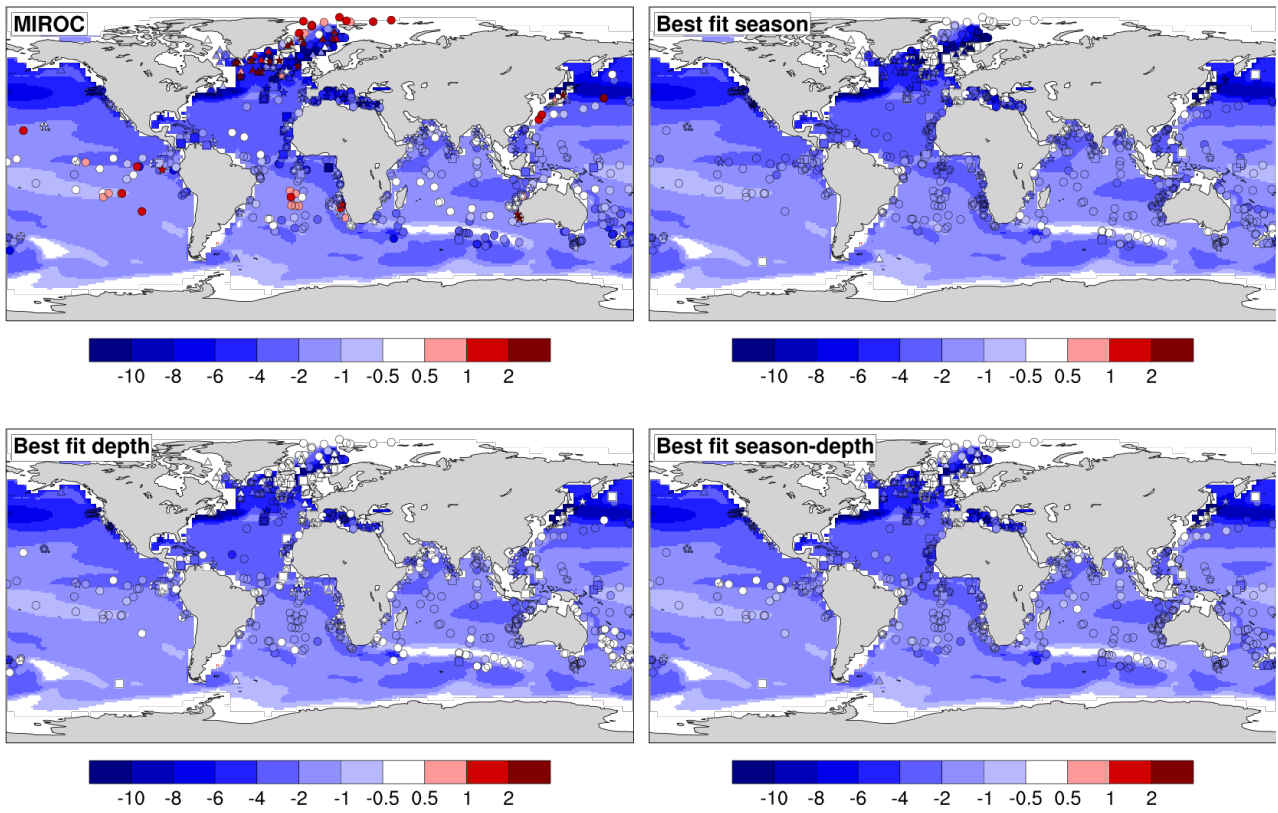


Fig. S9: As Fig. S5, but for MIROC.

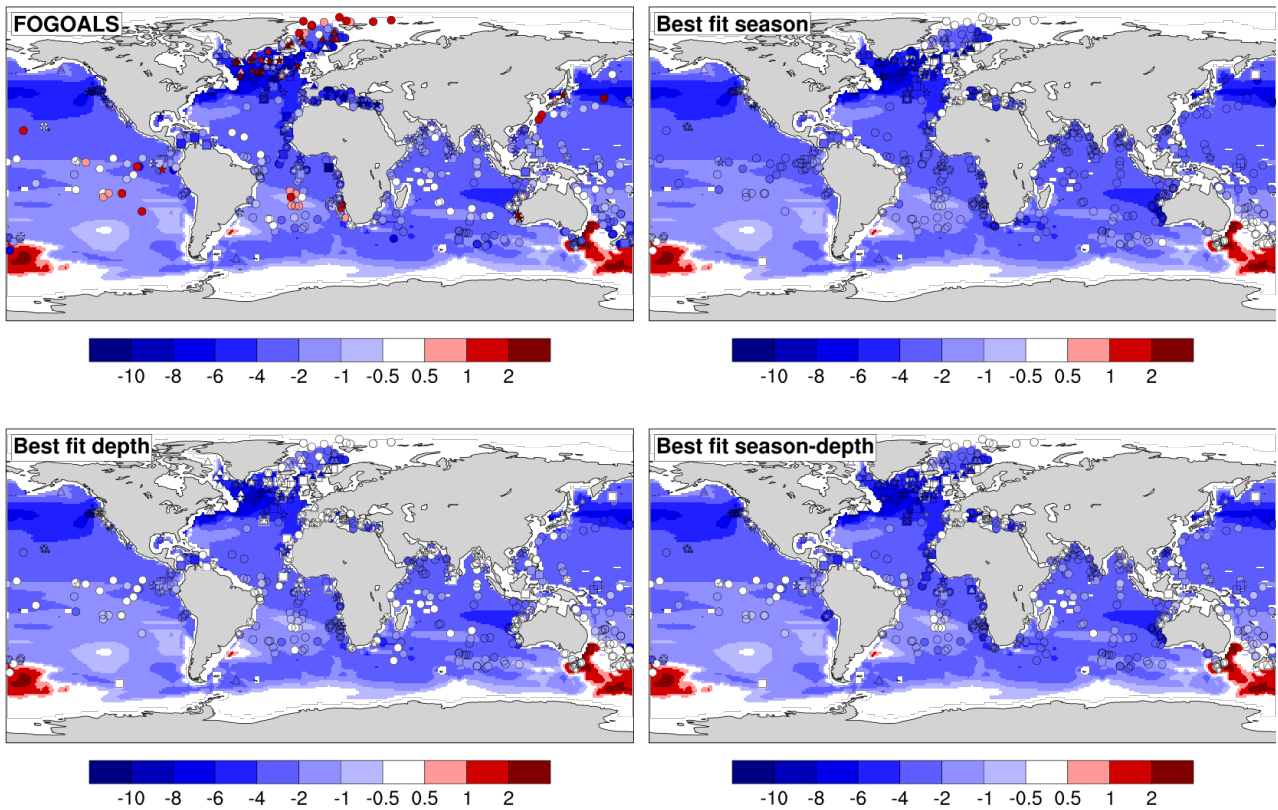


Fig. S10: As Fig. S5, but for CNRM.

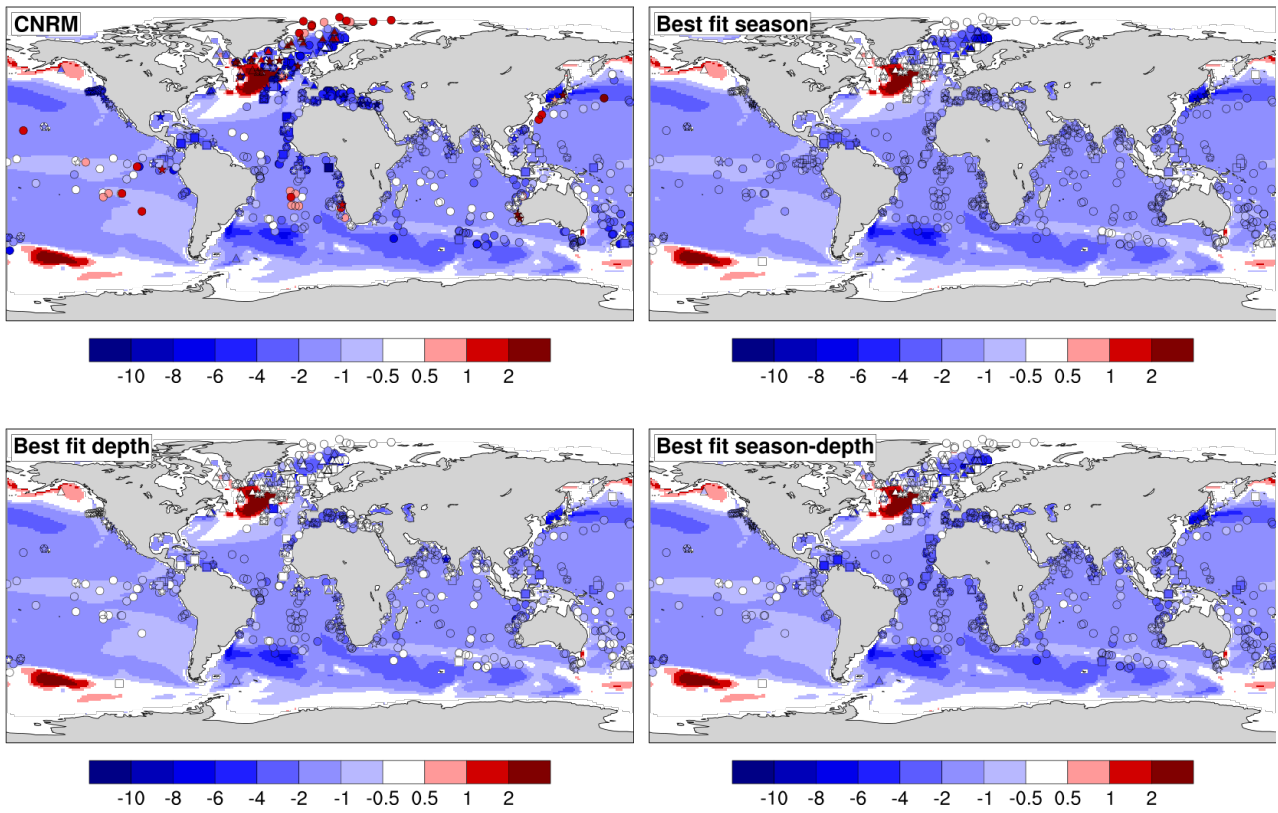


Fig. S11: As Fig. S5, but for FOGOALS.

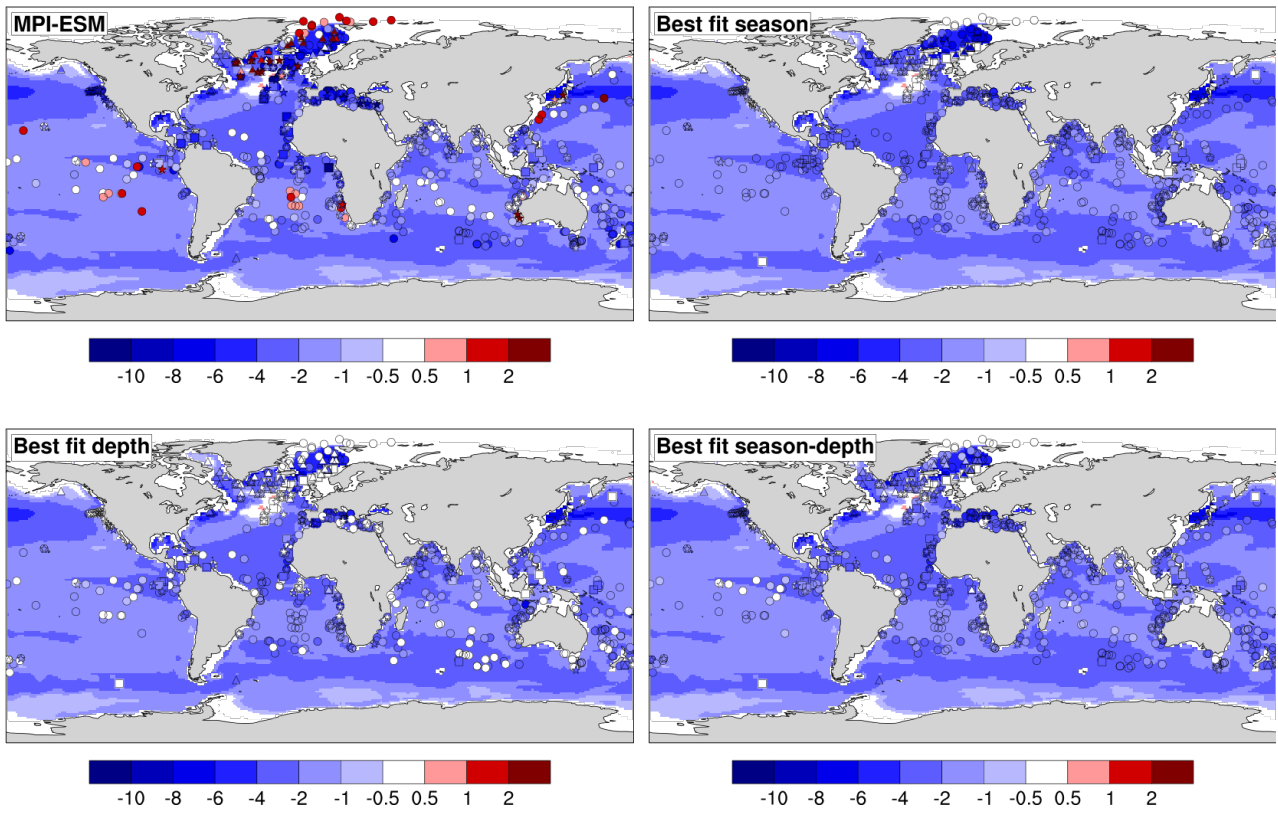


Fig. S12: As Fig. S5, but for MPI-ESM-P.

Table S1: PMIP3 Ocean-atmosphere coupled general circulation models used in this study.

Model	Abbreviated name	Oceanic resolution	References
IPSL-CM5A-LR ¹	IPSL-CM5A	2°×1.2°, L31	Dufresne et al. (2012)
MIROC-ESM ²	MIROC-ESM	1.4°×0.5°, L44	Watanabe et al (2011)
GISS-E2-R ³	GISS-E2	1.25°×1°, L32	Shindell et al. (2012)
CCSM ⁴	CCSM	1°×1°, L60	Gent et al. (2011)
FGOALS-G2 ⁵	FGOALS-G2	1°×1°, L30	Li et al. (2013)
MRI-CGCM3 ⁶	MRI-CGCM3	1°×0.5°, L51	Yukimoto et al. (2012)
CNRM-CM5 ⁷	CNRM-CM5	1°×0.6°, L42	Voldoire et al. (2012)
MPI-ESM-P ⁸	MPI-ESM	1.4°×0.8°, L40	Giorgetta et al. (2013)

¹Institute Pierre Simon Laplace Coupled Model version 5A-LR; ²Model for Interdisciplinary Research on Climate-Earth System Model; ³Goddard Institute for Space Studies Model E version 2 with Russell Ocean Model; ⁴ Community Climate System Model version 4; ⁵Flexible Global Ocean-Atmosphere-Land System Model, Grid-point Version 1.0; ⁶Meteorological Research Institute Global Atmosphere-Ocean Coupled Climate Model version 3; ⁷Centre National de Recherches Météorologiques Climate Model version 5; ⁸Max-Planck-Institute für Meteorologie Earth System Model.

Table S2: Correlation and RMSE between PMIP3 models annual mean SST and MARGO project dataset and MARGO proxies annual mean SST

	MARGO	Foraminifera	MgCa	Dinoflagellates	U ^k ₃₇
	R, RMSE				
IPSL-CM5A	0.32, 2.43	0.34, 2.59	0.25, 5.86	0.66, 3.76	0.33, 2.92
MIROC-ESM	0.27, 2.90	0.54, 2.37	0.62, 5.67	-0.08, 6.81	0.10, 3.55
GISS-E2	0.25, 2.51	0.44, 2.41	0.51, 5.68	0.51, 4.19	0.08, 3.21
CCSM	0.20, 2.64	0.48, 2.36	0.54, 5.93	0.23, 5.62	-0.06, 3.27
FGOALS-G2	0.13, 2.92	0.31, 2.76	0.41, 5.63	-0.22, 5.91	-0.32, 4.09
MRI-CGCM3	0.08, 39.35	0.10, 19.20	0.26, 5.66	0.21, 9.91	0.19, 23.46
CNRM-CM5	0.04, 2.68	-0.01, 3.10	0.18, 6.01	-0.12, 4.91	-0.07, 3.58
MPI-ESM	0.00, 2.70	0.25, 2.65	0.44, 5.96	-0.29, 5.42	-0.11, 3.34
Median_PMIP3	0.08, 39.25	0.11, 18.91	0.28, 5.55	0.19, 9.90	0.19, 23.45

Table S3: Correlation and RMSE between best-fit season of PMIP3 SST and proxies annual mean SST

	Foraminifera	MgCa	Dinoflagellates	U ^k ₃₇
	R, RMSE			
IPSL-CM5A	0.51, 2.31	0.38, 5.87	0.74, 3.13	0.54, 2.57
MIROC-ESM	0.12, 2.19	0.28, 5.62	0.29, 5.57	0.21, 2.98
GISS-E2	0.60, 2.21	0.64, 5.80	0.07, 3.28	0.38, 2.83
CCSM	0.47, 2.18	0.50, 5.82	-0.04, 4.78	0.22, 3.07
FGOALS-G2	0.57, 2.67	0.60, 5.77	0.74, 5.31	0.38, 3.78
MRI-CGCM3	0.59, 18.94	0.71, 5.62	0.36, 9.28	0.18, 23.11
CNRM-CM5	0.37, 2.80	0.55, 5.97	0.12, 4.23	-0.11, 3.25
MPI-ESM	0.30, 2.38	0.28, 5.87	0.19, 4.79	0.21, 3.03

Table S4: Correlation and RMSE between best-fit depth of PMIP3 SST and proxies annual mean SST

	Foraminifera	MgCa	Dinoflagellates	U^k_{37}
	R, RMSE			
IPSL-CM5A	0.50, 2.32	0.26, 5.90	0.68, 3.35	0.49, 2.66
MIROC-ESM	0.13, 2.06	0.27, 5.68	0.27, 4.09	0.22, 2.93
GISS-E2	0.65, 2.28	0.64, 5.86	0.31, 3.07	0.38, 2.37
CCSM	0.62, 2.20	0.51, 5.86	0.42, 4.24	0.37, 2.84
FGOALS-G2	0.60, 2.62	0.54, 5.82	0.74, 5.36	0.54, 3.73
MRI-CGCM3	0.60, 18.77	0.57, 5.60	0.41, 9.68	0.37, 23.04
CNRM-CM5	0.41, 2.67	0.46, 5.95	0.04, 4.14	-0.01, 3.11
MPI-ESM	0.38, 2.21	0.19, 5.88	0.24, 3.88	0.26, 2.85

Table S5: Correlation and RMSE between best-fit season & depth of COSMOS LIS SST and proxies annual mean SST

	Foraminifera	MgCa	Dinoflagellates	U^k_{37}
	R, RMSE			
LGMctl	0.70, 1.93	0.70, 5.61	0.42, 4.15	0.50, 2.69
Gowan	0.73, 1.83	0.76, 5.62	0.57, 3.84	0.52, 2.62
Ice6g	0.73, 1.85	0.73, 5.58	0.47, 4.20	0.43, 2.79
Lambeck	0.72, 1.88	0.75, 5.61	0.39, 4.36	0.45, 2.78
Licc	0.73, 1.83	0.78, 5.60	0.58, 3.87	0.50, 2.65
Tarasov	0.73, 1.82	0.74, 5.57	0.38, 4.34	0.44, 2.78
Median_LIS	0.73, 1.83	0.73, 5.61	0.43, 4.22	0.46, 2.73

Table S6: Correlation and RMSE between best-fit season & depth of PMIP3 SST and proxies annual mean SST

	Foraminifera	MgCa	Dinoflagellates	U^k_{37}
	R, RMSE			
IPSL-CM5A	0.63, 2.09	0.39, 5.85	0.78, 3.02	0.61, 2.43
MIROC-ESM	0.14, 1.89	0.29, 5.61	0.31, 3.85	0.23, 2.64
GISS-E2	0.72, 2.04	0.67, 5.79	0.43, 2.75	0.53, 2.54
CCSM	0.68, 1.99	0.48, 5.82	0.54, 3.91	0.52, 2.65
FGOALS-G2	0.68, 2.43	0.61, 5.77	0.81, 5.15	0.56, 3.58
MRI-CGCM3	0.70, 18.73	0.76, 5.57	0.53, 9.23	0.52, 23.00
CNRM-CM5	0.51, 2.49	0.52, 5.91	0.12, 3.79	0.08, 2.91
MPI-ESM	0.50, 2.05	0.30, 5.82	0.40, 3.65	0.40, 2.66

Reference

- Dufresne, J. L., Foujols, M. A., Denvil, S., Caubel, A., Marti, O., Aumont, O., Balkanski, Y., Bekki, S., Bellenger, H., Benshila, R. and Bony, S. (2013). Climate change projections using the IPSL-CM5 Earth System Model: from CMIP3 to CMIP5. *Climate Dynamics*, 40(9-10), 2123-2165.
- Gent, P. R., Danabasoglu, G., Donner, L. J., Holland, M. M., Hunke, E. C., Jayne, S. R., Lawrence, D.M., Neale, R.B., Rasch, P.J., Vertenstein, M. and Worley, P. H. (2011). The community climate system model version 4. *Journal of Climate*, 24(19), 4973-4991, <https://doi.org/10.1175/2011JCLI4083.1>.
- Giorgetta, M. A., Jungclaus, J., Reick, C. H., Legutke, S., Bader, J., Böttinger, M., Brovkin, V., Crueger, T., Esch, M., Fieg, K. and Glushak, K. (2013). Climate and carbon cycle changes from 1850 to 2100 in MPI-ESM simulations for the Coupled Model Intercomparison Project phase 5. *Journal of Advances in Modeling Earth Systems*, 5(3),

572-597.

- Li, L., Lin, P., Yu, Y., Wang, B., Zhou, T., Liu, L., Liu, J., Bao, Q., Xu, S., Huang, W. and Xia, K. (2013). The flexible global ocean-atmosphere-land system model, Grid-point Version 2: FGOALS-g2. *Advances in Atmospheric Sciences*, 30(3), 543-560.
- Shindell, D., Kuylenstierna, J. C., Vignati, E., van Dingenen, R., Amann, M., Klimont, Z., Anenberg, S.C., Muller, N., Janssens-Maenhout, G., Raes, F. Schwartz, J. (2012). Simultaneously mitigating near-term climate change and improving human health and food security. *Science*, 335(6065), 183-189.
- Voldoire, A., Sanchez-Gomez, E., y Méliá, D. S., Decharme, B., Cassou, C., Sénési, S., Valcke, S., Beau, I., Alias, A., Chevallier, M. and Déqué, M. (2013). The CNRM-CM5. 1 global climate model: description and basic evaluation. *Climate Dynamics*, 40(9-10), 2091-2121.
- Watanabe, S., Hajima, T., Sudo, K., Nagashima, T., Takemura, T., Okajima, H., Nozawa, T., Kawase, H., Abe, M., Yokohata, T. and Ise, T. (2011). MIROC-ESM 2010: Model description and basic results of CMIP5-20c3m experiments. *Geoscientific Model Development*, 4(4), 845.
- Yukimoto, S., Adachi, Y., Hosaka, M., Sakami, T., Yoshimura, H., Hirabara, M., Tanaka, T.Y., Shindo, E., Tsujino, H., Deushi, M. and Mizuta, R. (2012). A new global climate model of the Meteorological Research Institute: MRI-CGCM3—model description and basic performance—. *Journal of the Meteorological Society of Japan. Ser. II*, 90, 23-64.